RSC Advances

ROYAL SOCIETY OF CHEMISTRY

www.rsc.org/advances

Design of lamellar structured POSS/BPZ polybenzoxazine nanocomposites as the novel class of ultra low k dielectric material.

R. Sasi kumar, M. Ariraman and M. Alagar*

Polymer Composite Lab, Department of Chemical Engineering, A.C.Tech., Anna University, Chennai-600 025, India.

Abstract

A novel class of lamellar structured polyhedraloligomericsilsesquioxne/bisphenol Z (POSS/BPZ) polybenzoxazine nanocomposites was designed successfully via facile one step copolymerization technique. The chemical structure of monomer and resulting polymer were characterized by Fourier transform infrared (FTIR) spectroscopy, ^{1}H, ^{13}C, DEPT-135, ^{29}Si NMR (nuclear magnetic resonance) spectroscopy, X-ray diffraction (XRD), differential scanning calorimetric (DSC) and Thermogravimetric analysis (TGA). Desired cross linked lamellae structural arrangement of POSS/BPZ polybenzoxazine nanocomposites was confirmed with the transmission electron microscope (TEM). The BPZ-PBz and POSS-PBz layers were self-assembled by the intermolecular hydrogen bonding in such a way to form the lamellar structure during ring opening polymerization. In advantages to this lamellar structure, 30% POSS/BPZ polybenzoxazine composite exhibits ultra low k value of 1.7 at 1 MHz as well as high thermal stability.

Keywords: polybenzoxazine, POSS, lamellar structure, bisphenol Z, dielectric constant.

Introduction

Design of smart and miniaturized microelectronic devices such as, integrated circuits, memory devices etc., have been received enormous research interest owing to their negligible time delay which are necessary for ultra-fast electronic devices.[1] In general, the square of the dielectric constant is inversely proportional to the propagation velocity of the signal. Consequently, the high speed electronic device circuits require low-k material to realize the faster signal transmission without cross talk.[2,3] To achieve this, it is important to develop the

low-k dielectric materials that are been needed for the efficient integrated circuits. It is well established that the low-k silica and other related materials can prevent the signal cross over with low power consumption.[4] In this view, many efforts have been taken to reduce the dielectric constant (<1.8) with the different kind of materials.[5,6,7] Especially, nanolevel porous inorganic materials, variety of polymeric materials and their combinations are investigated for low-k dielectrics. At the same time, the low k composite materials should be compatible and have a strong adhesion with the improved thermal and mechanical stability. Based on these aspects, the composite materials of interconnected structures with air gaps and nanopores have been studied extensively. Widely, the networked polymers such as polyimide, POSS, PEEK, and Polybenzoxazine were reported for ultra low-k dielectric materials.[8-13]Among those POSS is one of the well known nanoporous inorganic material which contains eight organic groups with cubical structural arrangement and has been demonstrated to be an excellent building blocks for the high performance applications.[4]

Recent years, benzoxazine based organic-inorganic hybrid network structures have received a great research interest due to their unique structural, thermal and mechanical properties. The heterocyclic benzoxazine ring can be synthesized by Mannich condensation from phenolic derivatives, formaldehyde and primary amine. To the advantages of thermally induced ring opening addition polymerization of benzoxazine does not require any catalyst and there was no byproducts as well. In addition, the polybenzoxazine possesses an excellent thermal and mechanical properties, low moisture absorption, high carbon residue, low shrinkage and excellent electrical properties.[14] More importantly, the polybenzoxazine exhibits both inter and intra molecular hydrogen bonding in which the intermolecular hydrogen bonding could be beneficial for the self assembly of polybenzoxazine.[15] Hence, it is interesting to introduce the benzoxazine group into the porous polyhedral oligomeric silsesquioxane (POSS) compound for the preparation of self assembled polybenzoxazine nanocomposites to the benefit of reducing their value of dielectric constant. The pristine polybenzoxazine shows the dielectric constant in the range of ~3.5 and it can be used as an ideal dielectric material for microelectronics applications.[16] Meanwhile, the hybridization of benzoxazine with the ordered mesoporous materials such as POSS, SBA-15, SiO_2 reduces their value of dielectric constant as low as to ~2.[17-20] In addition to the above, their easy compatibility with the organic functional materials

like oxazole, fluorinated compounds, polyimide, etc, have increased their scope towards high performance applications.[12,14,16,21-23] Moreover, the characteristic polarization and favorable structural arrangement of functionalized polybenzoxazine reduces the dielectric constant greatly as low value needed for practical applications.[12,24] Liu et al reported the methylmethacrylate (MMA) and POSS hybrid composites with ordered lamellar structure and shows ultra-low k value of 1.47.[25] Further they have found that the lamellar arrangement plays the vital role to reduce the value of dielectric constant.[24-26] Similarly, Leu et al reported the POSS/Polyimide nanocomposites at the optimum of 29% POSS exhibits the dielectric constant of 2.3 when compared to that of neat Polyimide.[10] To the best of our knowledge there are no reports have been published till date with regard to lamellar structure based on POSS/BPZ-PBz nanocomposites. To the best of our knowledge there are no reports have been published till date with regard to lamellar structure based on POSS/BPZ-PBz nanocomposites. Specifically, 2-allyl phenol benzoxazine functionalized POSS with desired network structure have not been studied yet for low k dielectric applications. Hence, in the present work, an attempt has been made to develop a novel class of POSS/BPZ-PBz nanocomposites with an ordered lamellar structure by the copolymerization of polyhedral oligomeric silsesquioxane benzoxazine (POSS-Bz) and bisphenol Z benzoxazine (BPZ-Bz) in view to reduce the value of dielectric constant.

Experimental

Materials

Analytical grades of cyclohexanone, phenol, concentrated hydrochloric acid, acetic acid, aniline, paraformaldehyde, chloroform and toluene, were purchased from SRL, India. High purity tetraethylorthosilicate (TEOS), 2-allyl phenol, tetramethyl ammonium hydroxide (40% in methanol), chlorodimethylsilane, platinum (0)-1,3-divinyl-1,1,3,3-tetramethyldisiloxane complex solution in xylene [Pt (dvs)] catalyst were purchased from Sigma-Aldrich and were used as received without further purification.

Synthesis of 1,1-Bis(4-hydroxyphenyl)-cyclohexane (Bisphenol Z)

Typical synthesis of bisphenol Z (BPZ) are as follows; 10.37ml of cyclohexanone (0.22mol) was charged in to the mixture of concentrated hydrochloric acid and acetic acid (2:1 V/V), subsequently phenol (19.32ml, 0.1 M) was added dropwise to the reaction mixture and stirred for 48 h at 55 ^{o}C. The required amount of distilled water was added to the reaction mixture and resulting pink-colored product was isolated by filtration and washed several times with hot water to remove the excess phenol before dried at 70-80^{o} C. Finally, the end product was recrystallized using ethanol to obtain off white crystalline powder (Yield: 78%).

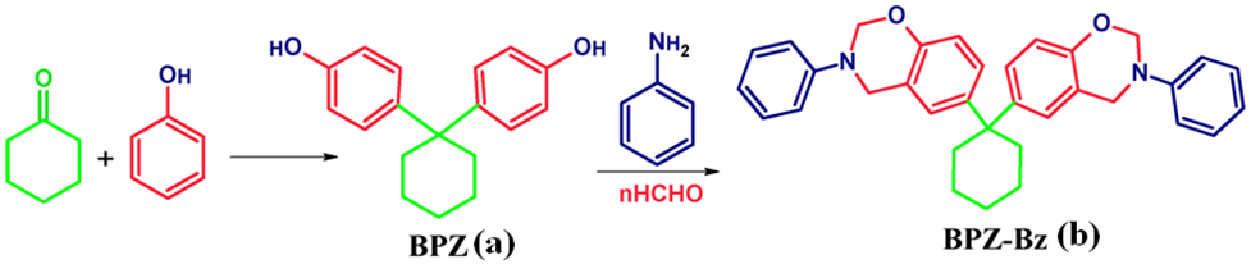

Scheme 1. Synthesis of BPZ (a) and BPZ-Bz (b).

Synthesis of bisphenol Z benzoxazine (BPZ-Bz)

To a solution of aniline (6.8ml, 0.075mol) in toluene, the formaldehyde (5g, 0.167mol) was added and stirred for 30 minutes at 0^{o} C. Followed by 10g of bisphenol Z (0.037mol) was added to the reaction mixture and stirred for overnight at 80^{o} C. After the completion of reaction (monitored by TLC), the reaction mixture was extracted with ethyl acetate and washed with 2N NaOH, water, brine and concentrated the organic layer to yield 95% brownish semi solid.

Synthesis of 2-allyl phenol benzoxazine (AP-Bz)

To a solution of aniline (5ml, 0.055mol) in chloroform, formaldehyde (3.3g, 0.11mol) was added and stirred for 30 minutes at 0^{o} C. Subsequently, 7.12 ml of 2-allyl phenol (0.055mol)

was added to the reaction mixture and stirred for overnight at 70° C. After the completion of reaction, the reaction mixture was extracted with ethyl acetate and washed with 2N NaOH, water, brine and concentrated the organic layer to yield 97% pale yellow liquid.

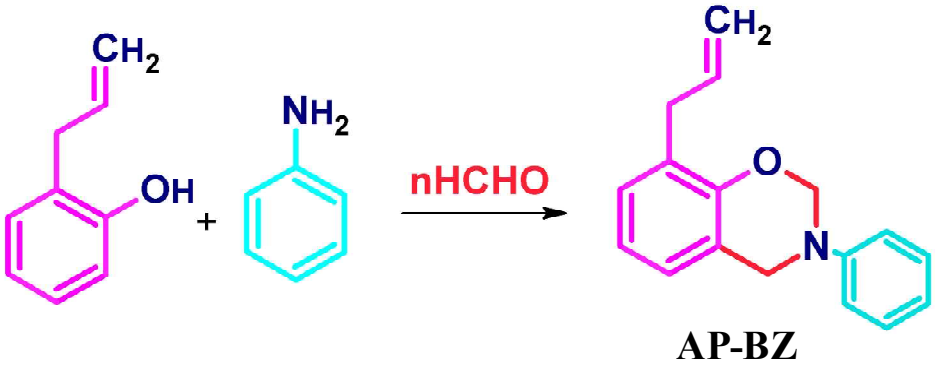

Scheme 2. Synthesis of AP-Bz.

Synthesis of OHC-POSS

The octahydridocubic polyhedral oligomeric silsesquioxane (OHC-POSS) was synthesized by the procedure as reported.[27,28] Octaanion solution $[Me_4N^+]_8[SiO^-_{2.5}]_8$ was prepared by mixing of tetra-methyl ammonium hydroxide (8.04ml), methanol (3.91ml), and de-ionized water (2.93ml) followed by dropwise addition of tetra-ethoxysilane (4.28ml) under nitrogen atmosphere. OHC-POSS $[HMe_2SiOSiO_{1.5}]_8$, was made by the reaction of octanion solution (18.5ml) with dimethylchlorosilane (10.6ml) to yield 38% of white crystalline powder.

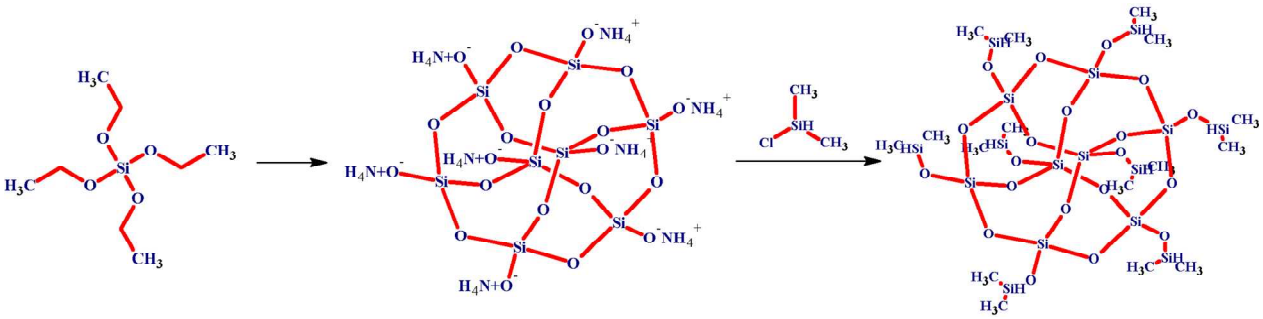

TEOS **Octanion intermediate** **OHC-POSS**

Scheme 3. Synthesis of OHC-POSS.

Synthesis of POSS-Bz

Finally, benzoxazine functionalized polyhedral oligomeric silsesquioxane (POSS-Bz) was synthesized by the addition of AP-Bz with OHC-POSS using Pt(dvs) catalyst. To a solution of OHC-POSS (10g, 0.009mol) in chloroform, Pt(dvs) catalyst (8 drops) was added under nitrogen atmosphere and stirred for 30 minutes at 30 ^{o}C. Subsequently the solution of AP-Bz (21g, 0.08mol) in chloroform was added to the reaction mixture and stirred for overnight at 110^{o} C. After the completion of reaction reduced the temperature to 30^{o} C and activated charcoal was added to the reaction mixture and filtered through celite, the filtrate was concentrated by the rotary evaporator to yield 91% of product as a pale yellow semi solid.

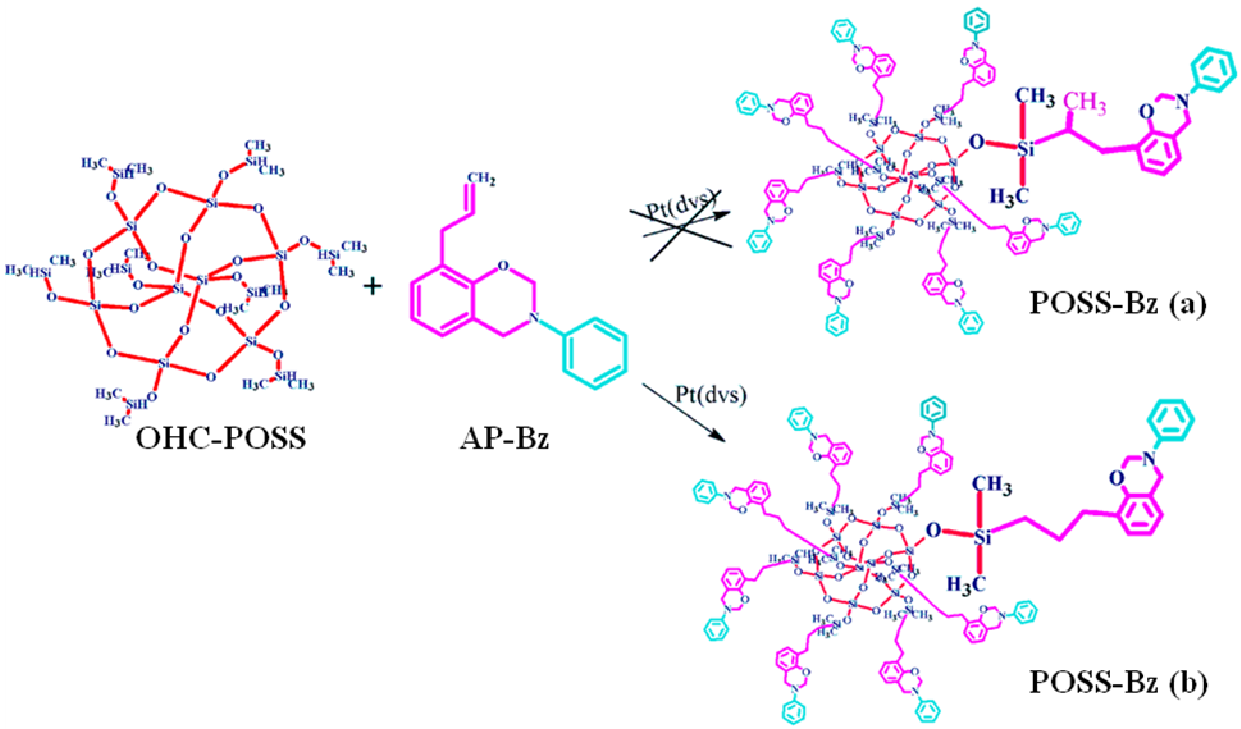

Scheme 4. Synthesis of POSS-Bz.

Preparation of neat polybenzoxazine matrix

In a glass mold, solutions of POSS-Bz and BPZ-Bz in tetrahydrofuran (THF) was separately heated at 100 °C for overnight to evaporate the solvent and then cured stepwise at 120, 140, 160, 180, 200, 220, 240 and 260 °C for 1h each to obtained dark brown film.

Preparation of POSS/PBz nanocomposites

The varying weight percentages of POSS-Bz (10, 20, 30, 40 and 50 wt %) were added to 2 g of BPZ-Bz dissolved in 10 mL THF. The resulting solution was stirred for 30 min at 30^{o} C. The solutions were poured into respective glass molds and were heated at 100° C for 3h and then cured stepwise at 120, 140, 160, 180, 200, 220, 240 and 260 °C for 1h each.

Characterization

^{1}H and ^{13}C NMR spectra were recorded on a Brucker-300 NMR spectrometer. ^{29}Si NMR spectra were obtained from a Brucker-500 NMR spectrometer. Fourier-transform infrared (FTIR) spectra of KBr disks were obtained using a Bruker Tensor 27 FT-IR spectrophotometer. The X-ray diffraction analysis of the samples were carried out using a Rigaku, miniflux II-C X-ray diffractometer (30 kV, 20 mA) with a copper target (1.54 Å) at a scan rate of 4°/min. Thermogravimetric and differential scanning calorimetric analyses of the polybenzoxazine films were carried out with a Exstar 6300 at a heating rate of 10 °C/min under nitrogen atmosphere. The surface overview of the composites was identified from FEI QUANTA 200F high resolution scanning electron microscope (HRSEM). Samples for the high resolution transmission electron microscopy (HRTEM) analysis were first prepared by putting POSS-Bz/BPZ-Bz nanocomposites films into epoxy capsules and cured at 70 °C for 24 h in a vacuum oven. After that, the cured epoxy samples were microtone with a Leica Ultracut Uct into about 100 nm thick slices and placed over the mesh of 200 copper nets. HRTEM images were captured using TECNAI G_2 S-Twin transmission electron microscope, with an acceleration voltage of 250 kV.

Results and discussion

Scheme 1a represents the synthesis route of bisphenol Z (BPZ) and the corresponding FT-IR spectrum is shown in Figure 1a. The appearance of peaks at 2931 cm^{-1}, 2853 cm^{-1} and 819 cm^{-1} are assigned to para-substituted benzene ring, symmetric and asymmetric stretching C-H bond respectively.[28] ^{1}H NMR spectra of BPZ (Figure 2a) shows the peaks at 8.25 ppm, 7.05-6.72 ppm and 2.17-1.46 ppm, associated to hydroxyl, aromatic and aliphatic cyclohexyl ring protons which confirms the successful formation of BPZ.

The Mannich condensation of BPZ and aniline to form BPZ benzoxazine monomer has been represented in Scheme 1b. From the FT-IR spectra as shown in Figure 1a, the bands related to tri-substituted benzene ring, (N-C-O), and (C-O-C) can be seen at 1508 cm^{-1}, 948 cm^{-1} and 1232 cm^{-1} respectively.[28,29] The ^{1}H NMR peaks at 5.31 ppm and 4.58 ppm in Figure 2b corresponds to (O-CH_2-N) and (Ar-CH_2-N) resonance of benzoxazine ring.

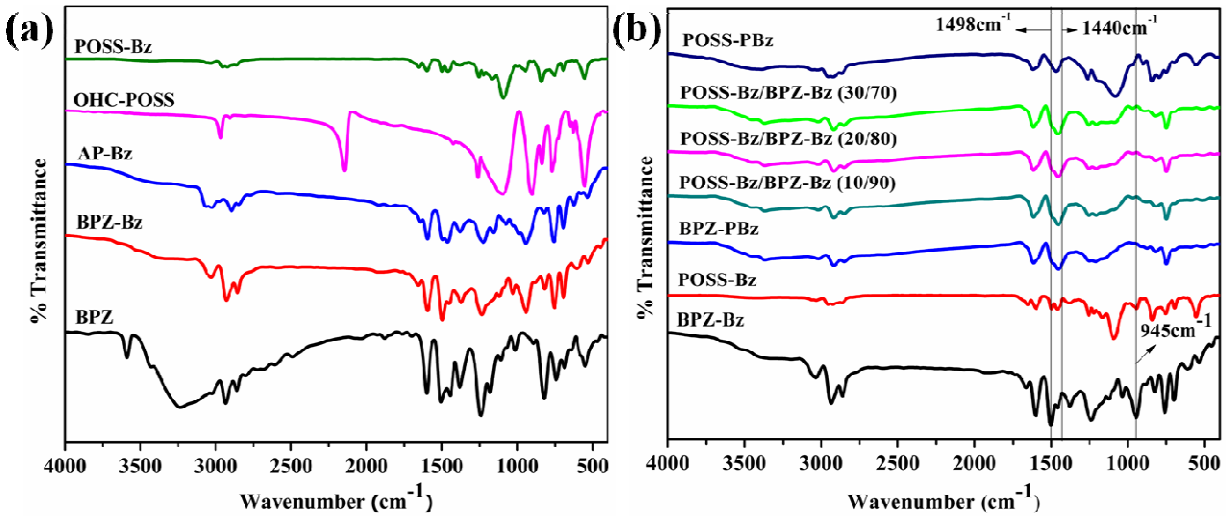

Figure 1. FTIR spectra of BPZ, BPZ-Bz, AP-Bz, OHC-POSS and POSS-Bz (1a) & POSS/BPZ-PBz polybenzoxazine nanocomposites (1b).

The AP-Bz was synthesized by the condensation of 2-allyl phenol with aniline as represented in Scheme 2. The FT-IR bands (Figure 1a) at 941 cm^{-1} (N-O-C) and 1221 cm^{-1} (Ar-C-N) confirms the formation of benzoxazine and it was further supported by the ^{1}H NMR peaks at 5.37 ppm (O-CH_2-N) and 4.62 ppm (Ar-CH_2-N) in the spectra as shown in Figure 3.

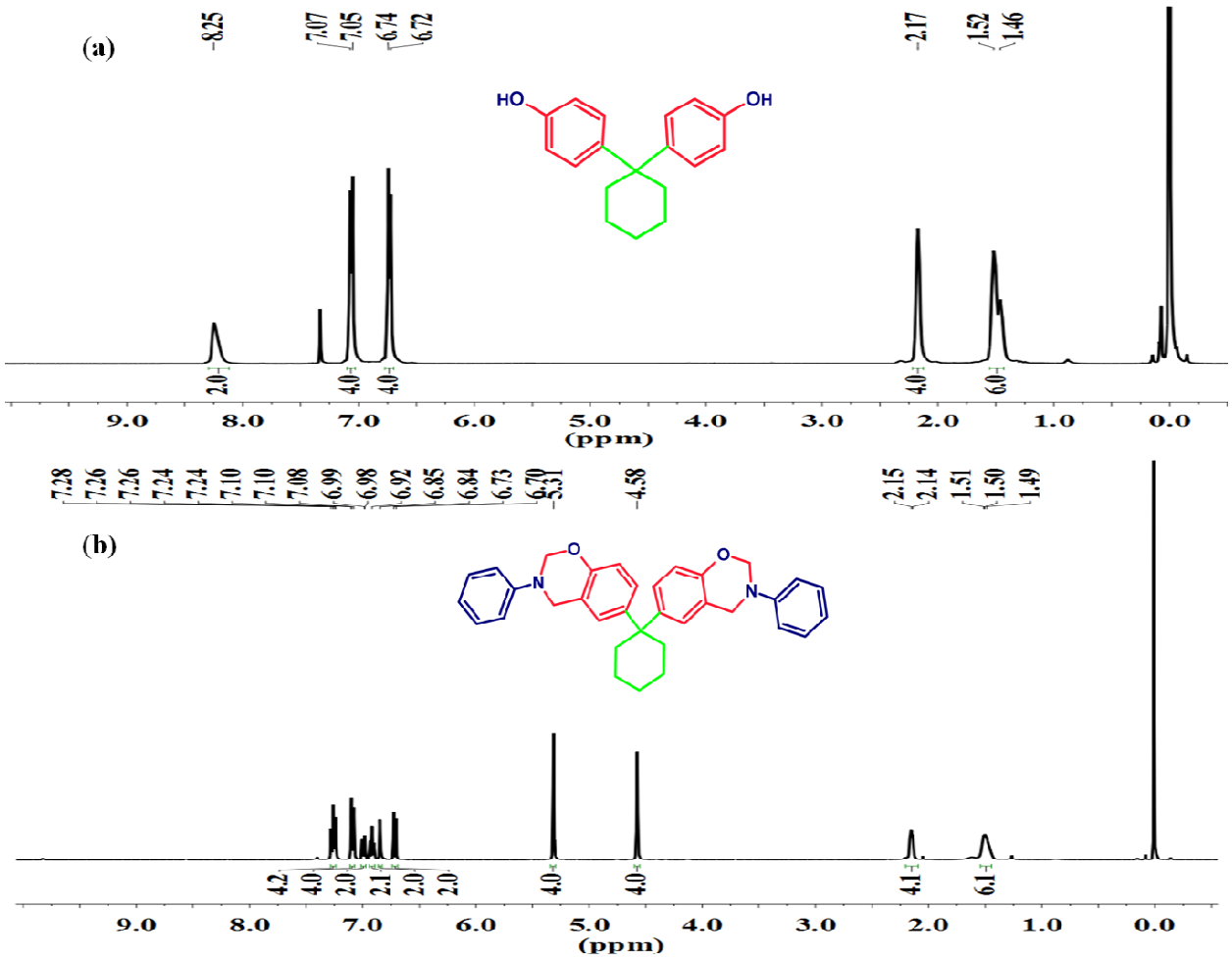

Figure 2. ^{1}H NMR spectra of BPZ (a) and BPZ-Bz (b).

The OHC-POSS preparation was shown in Scheme 3 and the chemical structure of the same was confirmed by FT-IR and ^{1}H NMR spectra as shown in Figure 1a and Figure 4b respectively. The strong FT-IR bands are positioned at 1097 cm^{-1}, 2145 cm^{-1} and 902 cm^{-1} associated to the Si-O-Si, Si-H stretching and bending vibrations of OHC-POSS.[20] The ^{1}H NMR

peaks appeared in the range of 4.74-4.72 ppm (Si-H), and 0.26-0.25 ppm [$Si(CH_3)_2$] as a multiplet, indicates the successful formation of OHC-POSS.

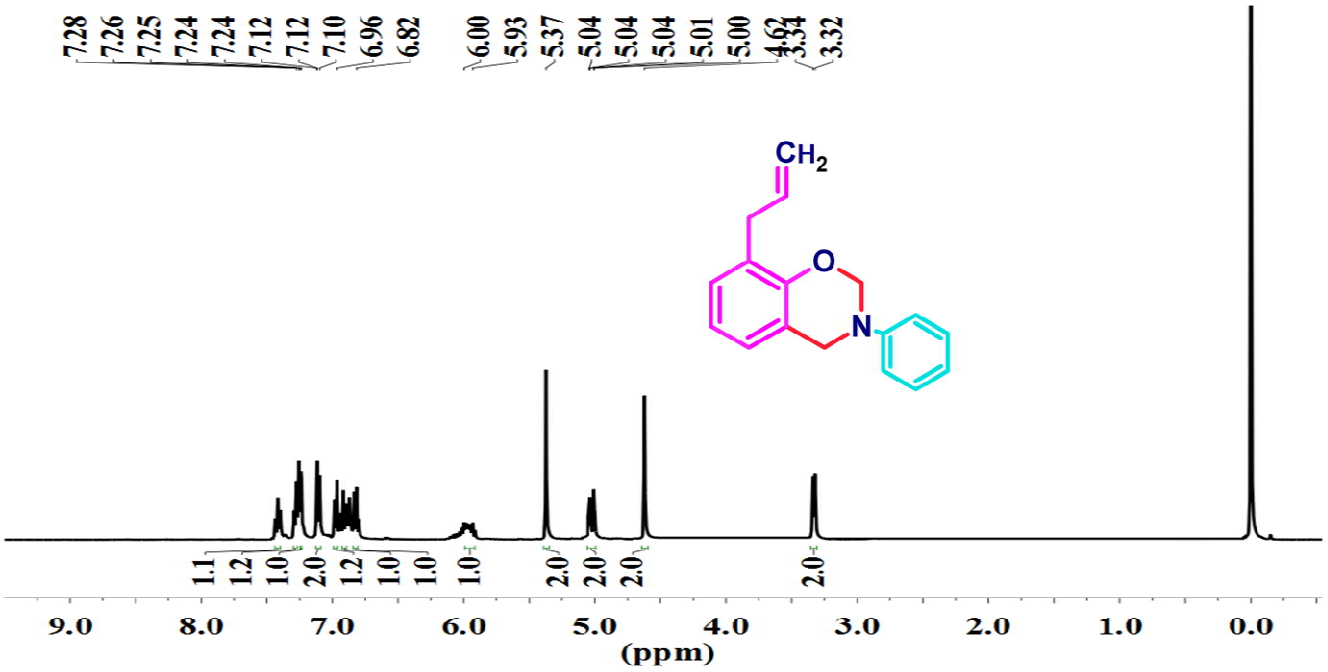

Figure 3. ^{1}H NMR spectra of AP-Bz.

Scheme 4 shows the addition reaction between AP-Bz and OHC-POSS. The appearance of new FT-IR bands at 1166 cm^{-1} (Si-CH_2-CH_2) and absence of Si-H at 2145 cm^{-1} in Figure 1a ascribes the addition reaction. The ^{29}Si NMR spectra as sown in Figure 5a ascertain that the presence of Si-O-Si (-102.95 ppm) and Si-$(CH_3)_2$ (18.78 ppm) in POSS-Bz.[30] The corresponding ^{1}H NMR shifts in the region of 1.59-1.57 ppm and 0.65-0.61 ppm are related to Si-CH_2-$\underline{CH_2}$ and Si-$\underline{CH_2}$ in POSS-Bz cages and are shown in Figure 5b. Herein the two way of addition is possible as shown in Scheme 4. The precise addition reaction has been confirmed with the ^{13}C and DEPT-135 NMR spectra and is illustrated in Figure 6 (a & b). The ^{13}C NMR spectrum of POSS-Bz shows all carbon related (C, CH, CH_2, CH_3) peaks but in DEPT-135 NMR shown only the CH and CH_3 peaks that are appeared opposite to the CH_2 peak except the C peak. In this case, the ^{13}C NMR peaks at 152.2, 148.5, 130.5 and 120.29, are attributed to respective aromatic C peaks which are not been observed in DEPT-135. Moreover, the DEPT-135 NMR shows five

CH_2 peaks in the aliphatic up-field region and six CH peaks in the aromatic down-field region. The absence of CH_3 peak in aliphatic region indicates the formation of POSS-Bz (b) [Scheme 4].

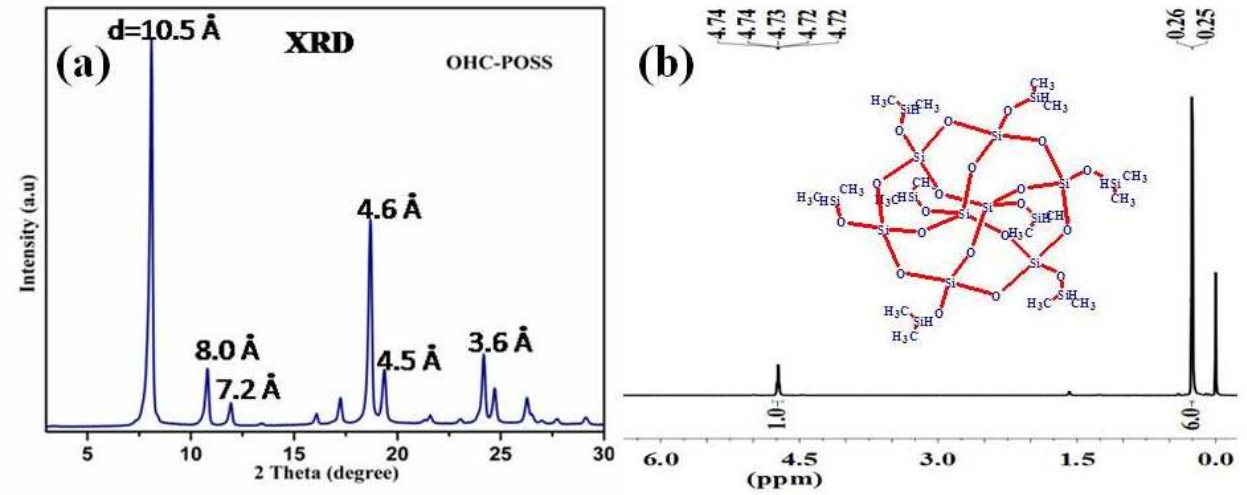

Figure 4. XRD pattern (a) and ^{1}H NMR spectra (b) of OHC-POSS.

The formation of polybenzoxazine nanocomposites were confirmed by FT-IR spectra. Figure 1b shows the FT-IR spectra of polybenzoxazine nano composites. The characteristic absorption bands at 945 cm^{-1} (out of plane bending vibration of C−H) and 1463 cm^{-1} (tri-substituted benzene ring) were gradually disappeared. Meanwhile, a new absorption band appeared at 1412 cm^{-1} is attributed to tetra-substituted benzene ring, indicates the ring-opening polymerization of benzoxazine.[28] It is further evidenced by the DSC analysis and described in detail at the thermal analysis section.

The stepwise structural modifications of POSS-Bz copolymer has been investigated by low angle X-ray diffraction pattern. Figure 8 shows the XRD patterns of respective POSS-Bz monomers and their conjugated polymers. From the pattern it can be seen that OHC-POSS exhibits (Figure 4a) highly crystalline features. It is that the peak positions and corresponding d-space values are found to 8.01°, 10.72 °, 11.86 °, 18.61 °, 24.1 ° and 10.5Å, 8.0 Å, 7.2 Å, 4.6 Å, 3.6 Å respectively. These values can be indexed to rhombohedral crystal structure and are in good agreement with the earlier reports as well.[10] In contrast, the benzoxazine monomer shows the predominant amorphous phase (Figure 8). Also, there is no

evidence for any crystalline phase for POSS-Bz monomer. This result further confirms the functionalization of AP-Bz with OHC-POSS which disrupts the crystallinity of OHC-POSS to a significant extent. However, copolymerization of POSS-Bz with BPZ-Bz shows different

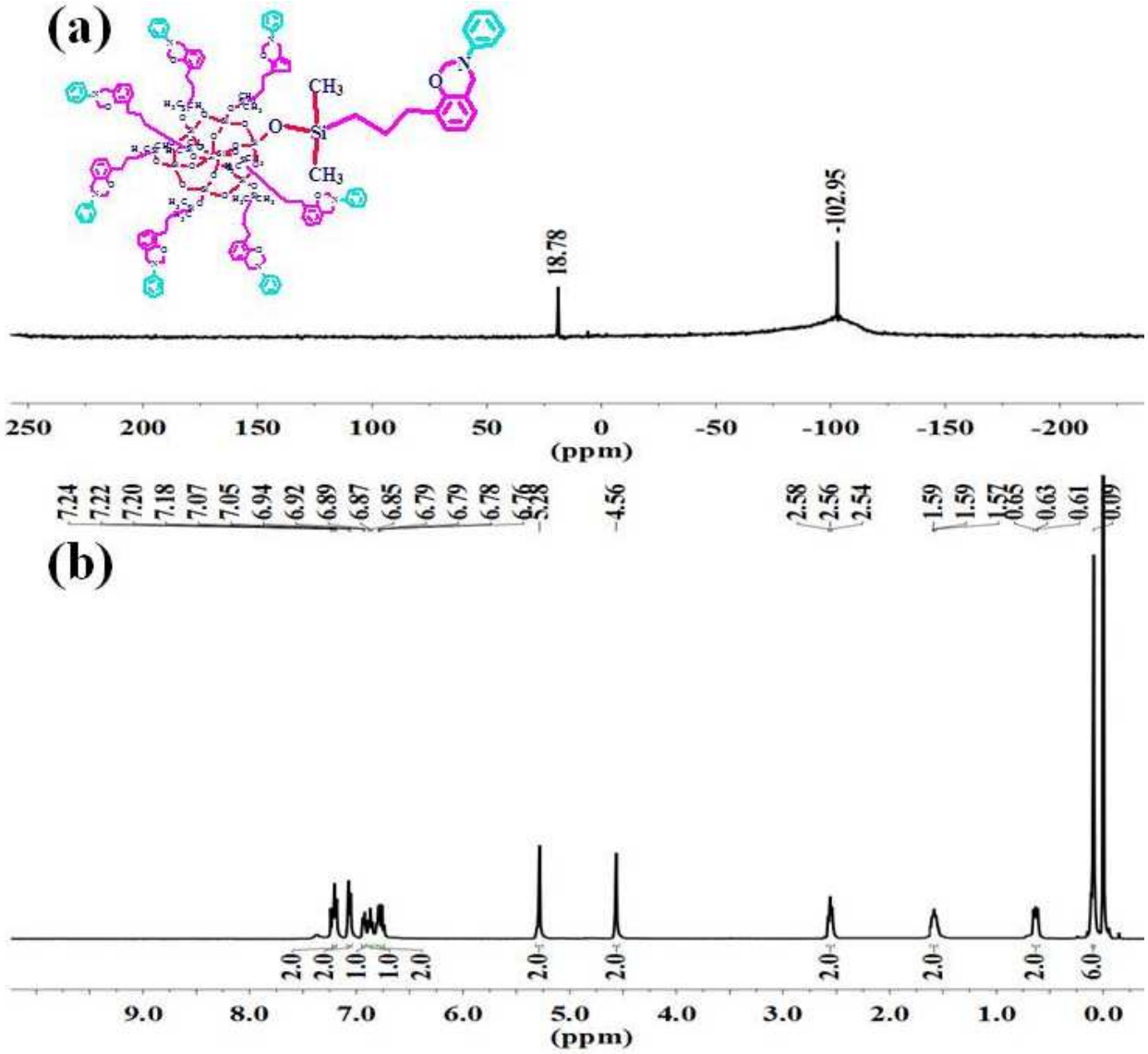

Figure 5. ^{29}Si (a) and ^{1}H NMR (b) spectra of POSS-Bz.

diffraction pattern as can be seen in Figure 8. With the concentration of POSS-Bz their crystallinity enhances, in particular 30% of POSS-Bz hybridized polymer composites have shown the higher crystallinity that may lower its dielectric constant to an extremely low value by

the benefit of their desired structural arrangements. This observation is in consistent with the earlier reports.[10,12] When increases the POSS-Bz concentration to above 30%, the crystallinity of the composites falls down towards amorphous due to the aggregation of POSS-PBz.

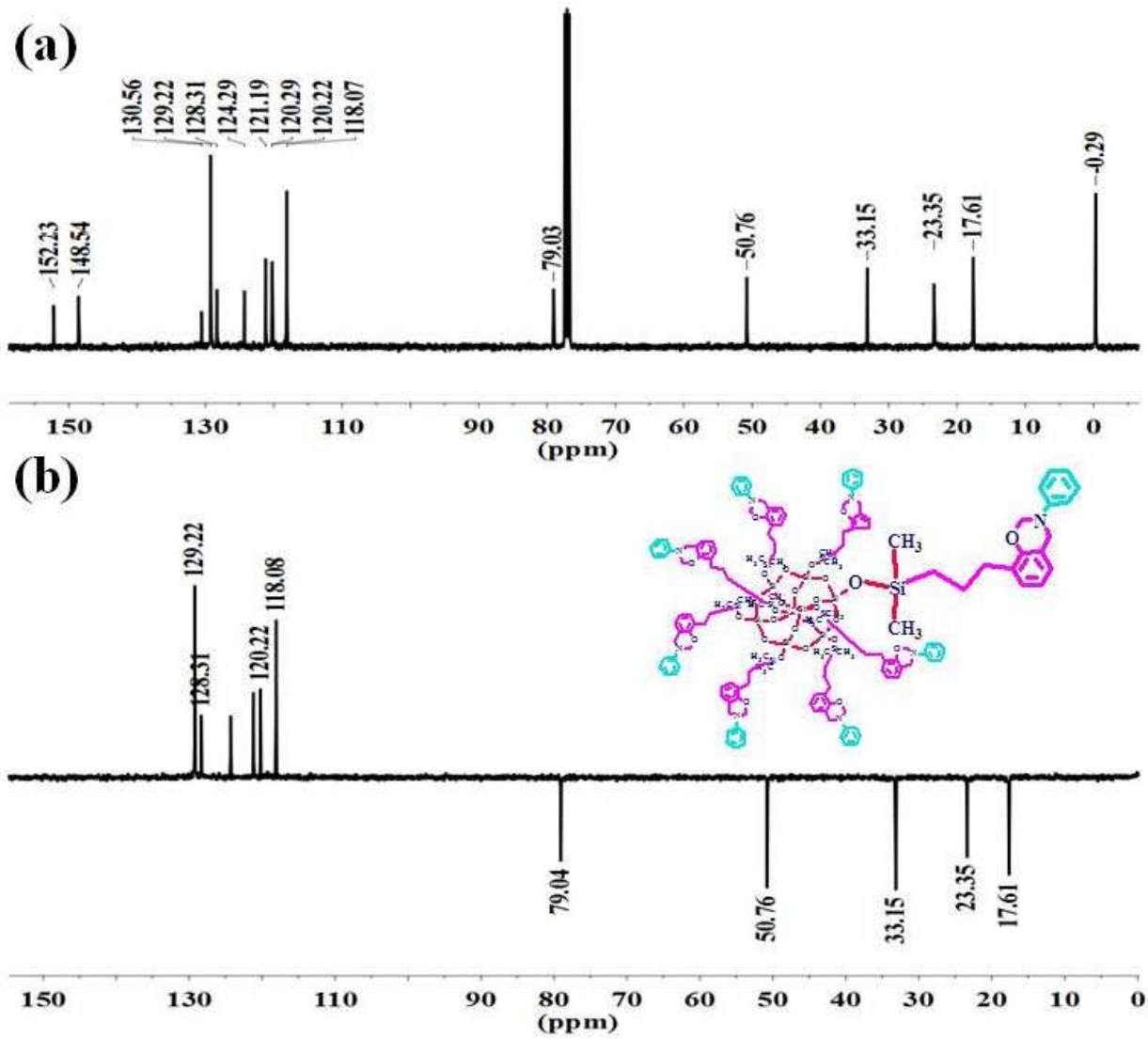

Figure 6. ^{13}C (a) and DEPT-135 NMR (b) spectra of POSS-Bz.

In order to understand the surface over view and the incorporation of POSS-Bz in the polymer network, the samples were analyzed by scanning electron microscope (SEM). Figure (9a-d) represents the SEM micrograph of neat BPZ-Bz (Figure 9a), 30% POSS/BPZ-PBz

(Figure 9b), the corresponding Si mapping (Figure 9c) and 100% POSS-PBz (Figure 9d). As can be seen that the dense morphology with large number of voids in the SEM micrograph of pristine BPZ-PBz film. It is mainly arises from the ring opening polymerization of cyclohexyl ring functionalized BPZ-Bz that enhances the external porosity of the neat as well as composite polymers. After the copolymerization process, the SEM image designates the uniformly distributed crystallite aggregates of POSS-Bz, in addition to the voids created by the BPZ-Bz. Moreover, the visible (Figure 9) open pores with dark background at 30% POSS-Bz composite film further increases the free volume space which also reduces the dielectric constant.[32,33] Conversely, the 100% POSS-PBz film have shown the large amount of crystallite aggregates are discernible when compared to that of 30% POSS-Bz composite. Figure 9c describes the results of Si-mapping for the 30% POSS-Bz composite and demonstrates that the uniform distribution of POSS-Bz over the surface.

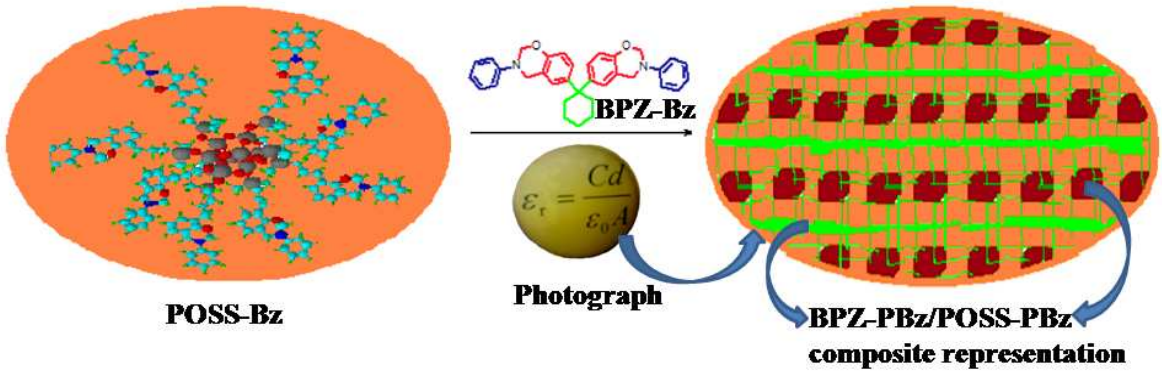

Figure 7. Schematic representation of BPZ/POSS Polybenzoxazine nanocomposites with cross linked lamellae and its photograph of film.

The internal microstructure of the 30% POSS-Bz composite film has been observed with the HRTEM analysis and the captured images are shown in Figure (10a, b & c). The TEM images are clearly indicating the ordered lamellae structure with multilayers. From the high magnification TEM as shown in Figure (10b & c) it can be seen that the well separated unidirectional multilayer's arrangement with large number of cross links. It could be understandable that the observed dark layers are associated to the POSS-PBz and the less intense layer corresponds to the BPZ-PBz. In this order the layers have been arranged and form the

desired lamellae structure.[10,12] During the ring opening copolymerization process, there is the more probability for the formation of hydrogen bonding which may self assemble the BPZ-PBz and POSS-PBz layers together, consecutively it forms the ordered lamellae.

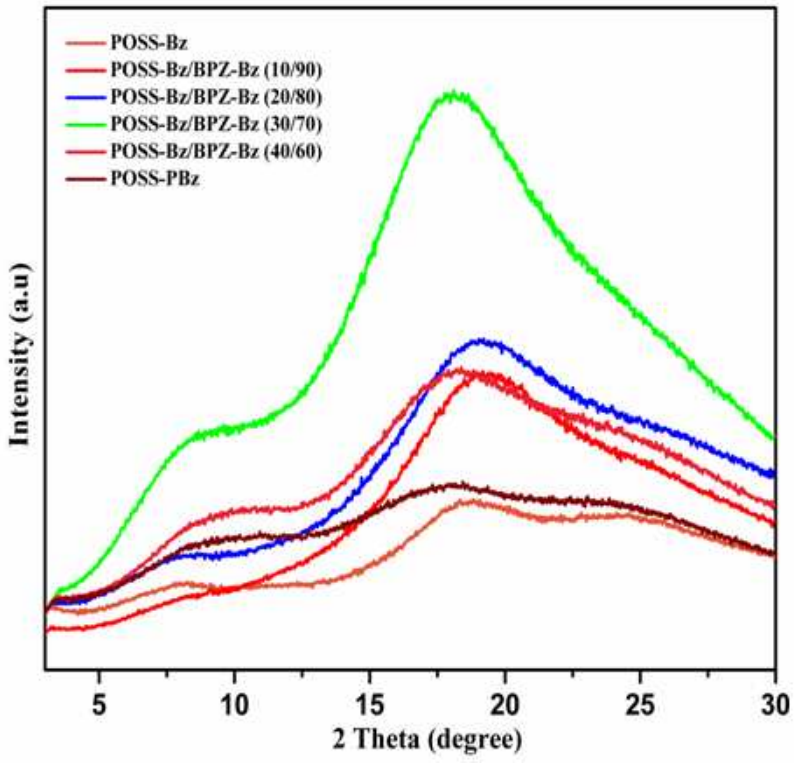

Figure 8. XRD pattern of pristine and POSS-Bz copolymerized nanocomposites.

Thermal stability is one of the important factors for the inter layer dielectric materials. Herein, the thermal stability of BPZ-Bz and POSS-Bz polymer nanocomposites has been studied with thermogravimetric analysis. Typical TGA curves of pristine and composite films are shown in Figure 11. As expected the BPZ-Bz copolymerized with POSS-Bz exhibits high thermal stability than the pristine. It is directly associated to the presence of POSS network strengthens the BPZ-Bz chains during copolymerization. When increases the POSS concentration it is observed that the gradual increment of thermal stability for the resulting composites. Although, the maximum thermal stability for POSS-PBz was obtained, this may be attributed to the formation complete stable POSS network.[14] In detail, the initial weight loss in the range of 240-300^{o} C probably by the removal of solvent residues. The major weight loss beyond 300^{o} C is associated to the degradation of polymer network which is in consistent with the earlier

investigation.[34] Typical DSC profile of the monomer shows (Figure 12a & b) the broad exothermic peak at above 175 °C as the indication of BPZ-PBz curing temperature. With the 30% POSS, only a single exothermic peak maximum at 224 °C was observed which indicates the co-reaction between the oxazine rings of POSS-Bz and BPZ-Bz.[14,35]

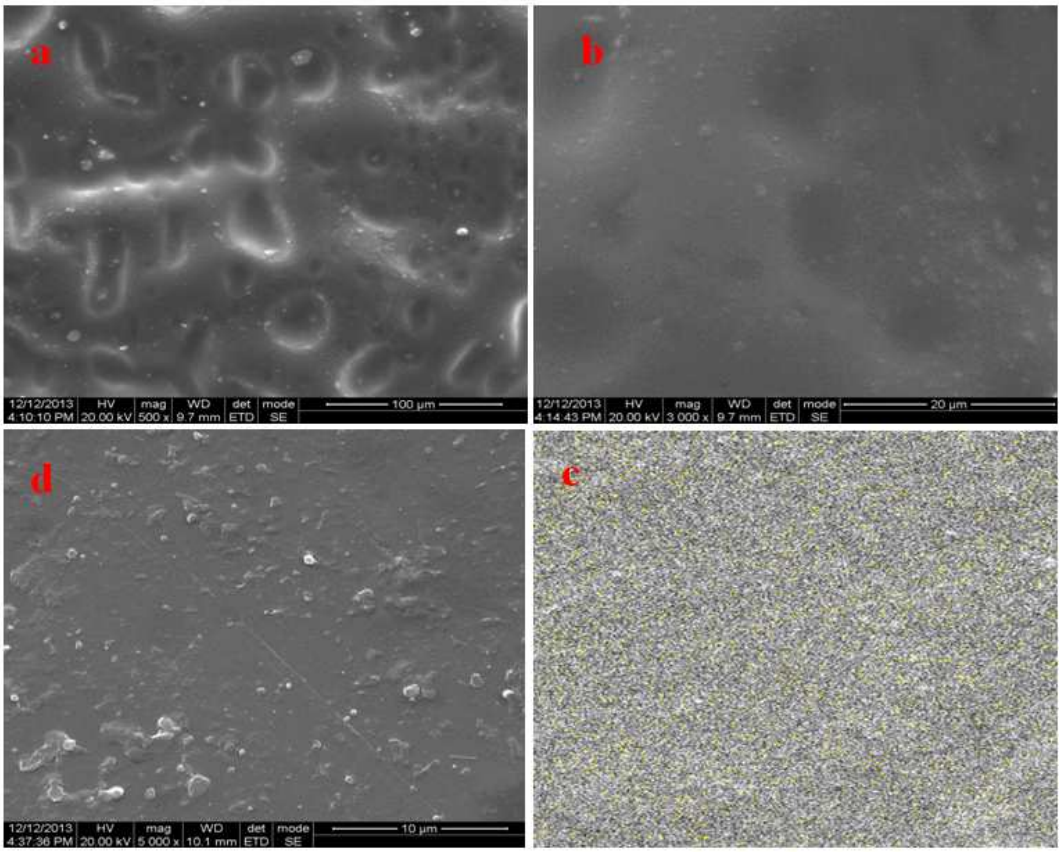

Figure 9. SEM images of BPZ-PBz (a), 30% POSS/BPZ-PBz (b), Si mapping of 30% POSS/BPZ-PBz (c) and POSS-PBz (d) nanocomposites.

In microelectronics applications the material with extremely low dielectric constant is more desirable and it warrants the development such novel materials. The extensive efforts are made by several researchers in order to reduce the dielectric constant nearly equivalent to air (1).[25,36] Generally, the polymer systems which offers the low k value should scarifies the other structural, chemical and thermal properties. Therefore it needs more concern to use the materials in full potential for commercial appliances. It is well established that the dielectric constant is a

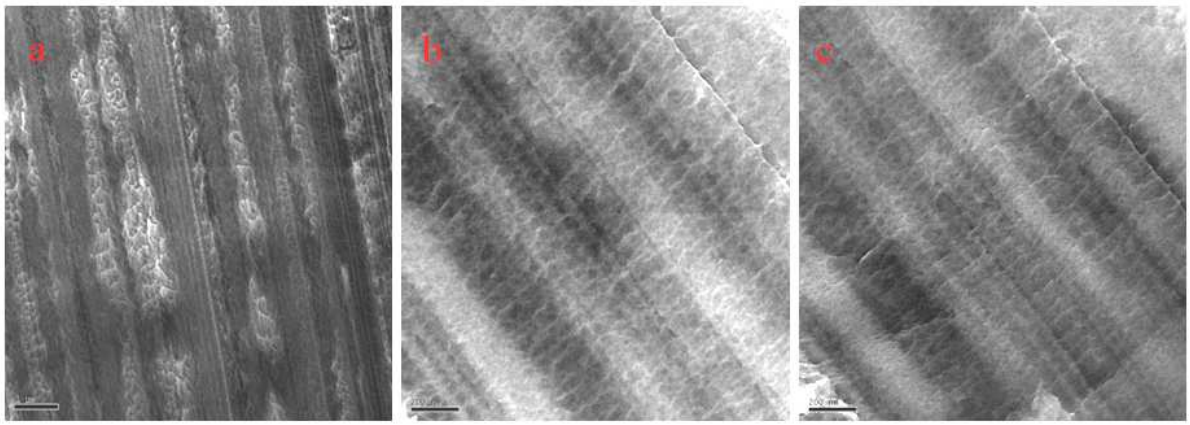

Figure 10. HRTEM micrographs for 30% POSS-Bz/BPZ-Bz polymer nanocomposites (a-1µm & b, c-200nm).

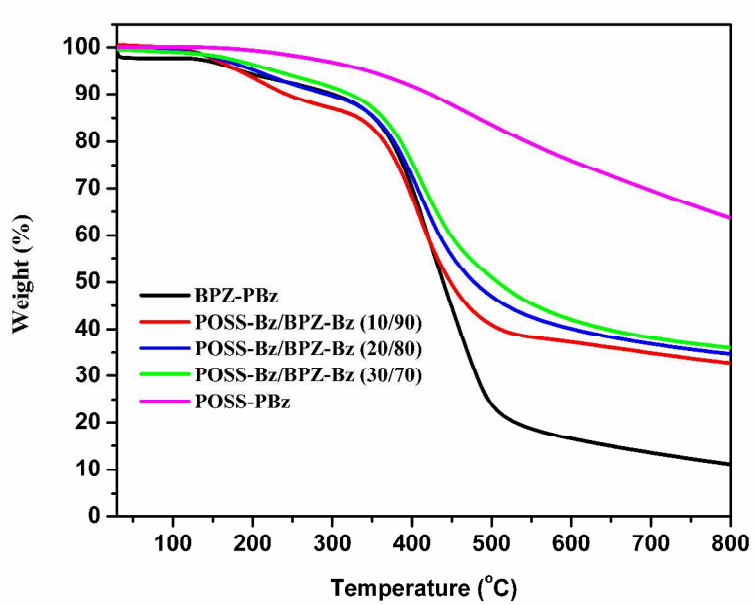

Figure 11. TGA curve of BPZ-PBz and POSS-PBz nanocomposites.

tunable factor and it can be possible by the introduction of mesopores in the polymer matrix which results lowering the value of dielectric constant at the extreme level upto ~1.7. Similarly, it can also be possible to reduce the dielectric constant by altering the chemical and physical structures of the polymer matrix using functionalization processes.[14,16,21] The former method lead by the mesoporous materials such as POSS, SBA-15 etc., which creates the pores in the polymer

matrix thus lowering the dielectric constant to a significant extent.[10,20] The later method requires the tedious synthesis process to alter the structure.

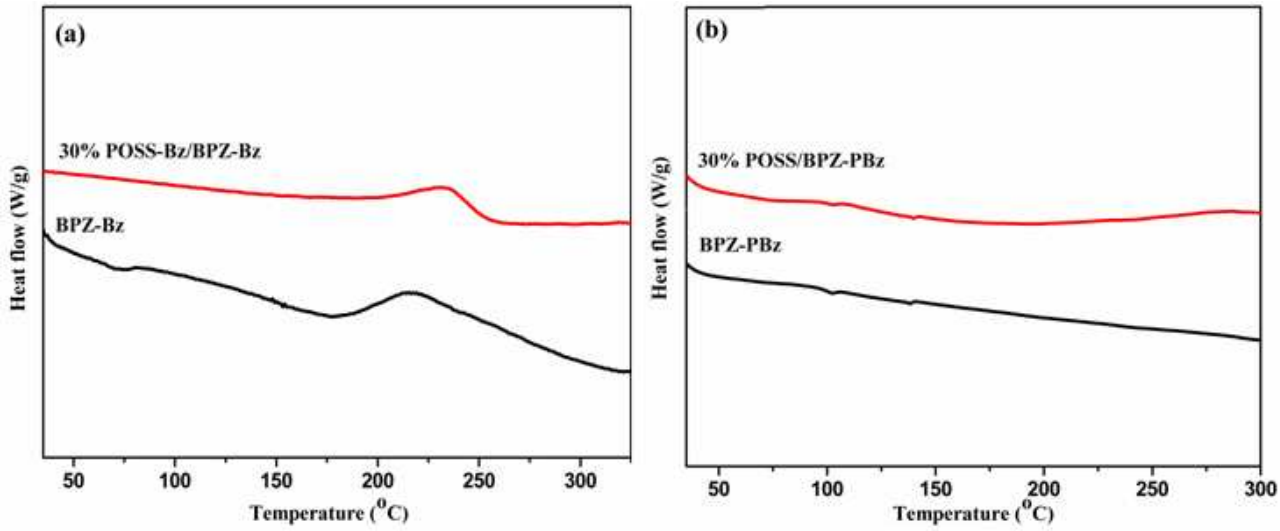

Figure 12. DSC profile of BPZ-Bz and 30%POSS/BPZ-Bz nanocomposite before (a) and after (b) polymerization.

According to the earlier reports on benzoxazine based nanocomposites exhibits the dielectric constant of about ~1.8 and it needed to be improved for better applications.[37] In this study, we designed a novel POSS/BPZ-PBz composite film with layered microstructure and has achieved the ultra low dielectric constant value of 1.7±0.01 at the optimum concentration of 30% POSS/BPZ-PBz nanocomposites (Table 1). To the best of our knowledge this is the lowest value for ever reported in the case of POSS/BPZ-PBz hybrid nanocomposites. This is the lowest value for ever reported in the case of POSS/BPZ-PBz hybrid nanocomposites. The novel type of 2-allyl phenol benzoxazine functionalized POSS plays the crucial role to impart desired lamellar structure which inturn contributes to result Ultra low-k value of the hybrid composites. An interestingly, the neat polymer shows the relatively low k value of 3.49 which is also comparatively lower when compared to that of the values reported earlier.[16,17,38] This may be due to the presence of larger voids that enhances the external porosity which in turn reduces the k- value considerably. In the present composite systems, when an increase in the concentration of POSS-Bz, the corresponding k-value decreases upto 30 weight% further it increases with increase in

concentrations. The neat POSS-PBz exhibits the higher value of dielectric constant of 2.9 than that of concentrations due to large aggregates of POSS crystallites and completely packed voids.

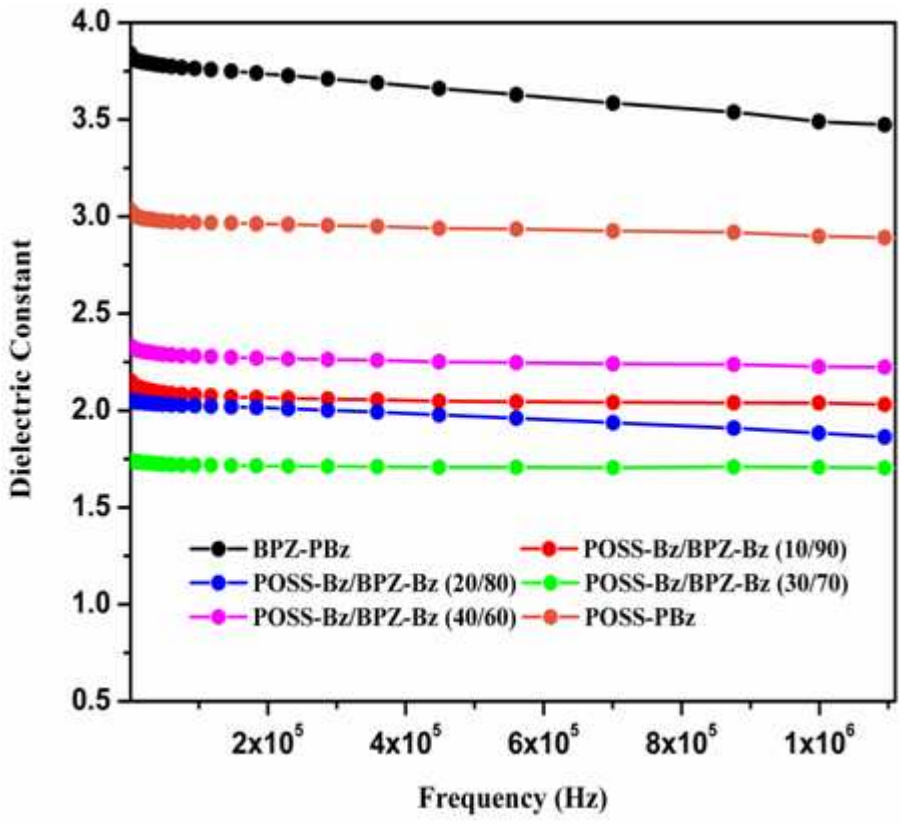

Figure 13. The frequency dependence of dielectric constants of BPZ-PBz and POSS-PBz nanocomposites.

The observed ultra low k (Figure 13) for the POSS/BPZ-PBz composites can be explained by the following structural features; first, the self assembled layered structure with unidirectional orientation is responsible for reducing the polarization by increasing an inter and intra layer distances.[12,24-26]In particular, the layer thickness for the dark region (POSS-PBz) is higher when compared to that of the BPZ-PBz layer and it is almost two order magnitude that increases the internal porosity due to the high volume fraction of POSS density in the film. Therefore, the reduction in dielectric constant is strongly influenced by POSS portion in composites. At 30% POSS-Bz concentration imparts the desired lamellae structure with enhanced crystallinity which in turn results the ultra low k value at this concentration.

Sample	T5 (^{o} C)	T10 (^{o} C)	Yc (%)	Dielectric constant (k)
BPZ-PBz	186.2	301.2	11.2	3.49±0.01
10%POSS-Bz/BPZ-Bz	184.0	242.8	32.8	2.03±0.01
20%POSS-Bz/BPZ-Bz	204.6	294.0	34.7	1.86±0.01
30%POSS-Bz/BPZ-Bz	229.3	322.5	36.1	1.70±0.01
POSS-PBz	345.7	423.7	63.8	2.89±0.01

Table 1. The weight loss, char yield (Yc) and dielectric constant (k) of neat BPZ-PBz and POSS/BPZ-PBz nanocomposites.

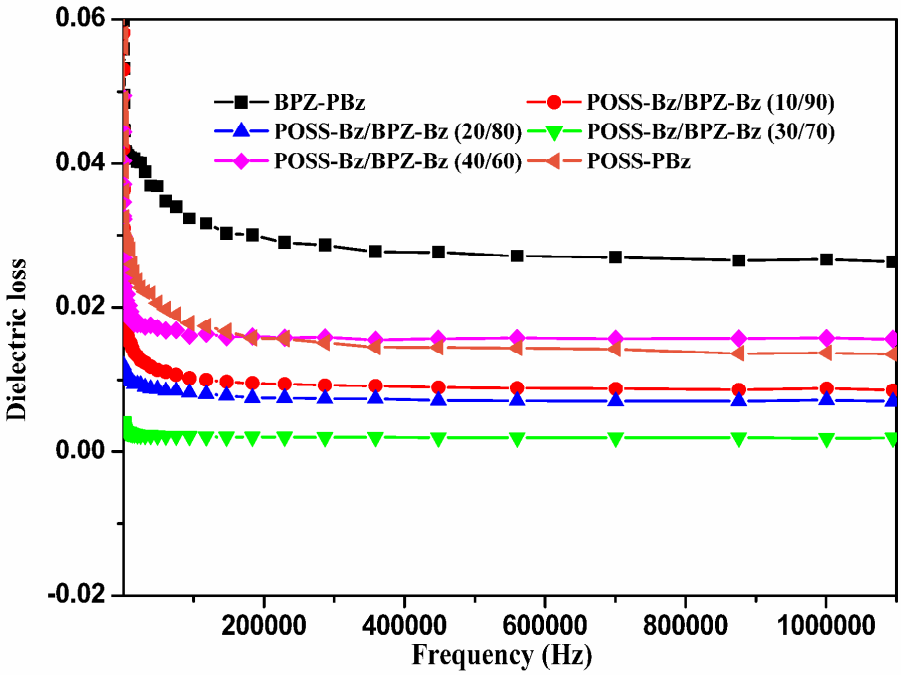

Figure 14. The frequency dependence of dielectric loss of BPZ-PBz and POSS-PBz nanocomposites.

In addition, the cyclohexyl functionalized benzoxazine monomer (BPZ-Bz) offers the external voids to enhance the free volume of the composite that also play the significant role to reduce the value of dielectric constant. Further an increasing the percentage of POSS

concentration upto 100%, the larger aggregation and lower crystalline features enhances the value of dielectric constant due to reduction of voids and dense packing. Dielectric loss is a one of the key factor to understand the utilization of dielectric material in microelectronics. Typical frequency versus dielectric loss curves of the POSS/BPZ polybenzoxazine nanocomposites are shown in Figure 14. It is found that the observed dielectric loss is ultimately very low in the value of 0.0019 at 1MHz for lamellar structured 30% POSS-Bz composites which shows the ultra low k value as well. From this investigation it is suggested that the design and introduction of lamellar structure in to the POSS/BPZ-PBz hybrid nanocomposites could be effectively used as an interesting candidate for the microelectronic devices.

Conclusion

In view to reduce the dielectric constant, we successfully designed the novel hybrid POSS/BPZ polybenzoxazine nanocomposite systems. As expected the composite with 30% POSS exhibits the ultra low k value of 1.7±0.01 at 1MHz. The observed low k value mainly attributed to the highly ordered lamellar network with distinct cross links. Meanwhile, the thermal stability and dielectric constant has been tuned by varying the POSS concentration without loss of their transparency. This kind of hybrid composites can expect to find potential application in advanced microelectronic devices.

Supplementary Information: Data's of FTIR and NMR spectra are provided for more information.

Acknowledgement:

The authors thank DST Nanomission, (SR/NM/NS-18/2010), New Delhi, Govt. of India., for the financial support. The authors thank Dr. K. Gunasekaran and Mr. M. Kesavan, Dept. of Crystallography and Biophysics, University of Madras, for providing the NMR facility.

References

1. Y. Huang and J. Economy, *Macromolecules*, 2006, **39**, 1850-1853.
2. Y. Watanabe, Y. Shibasaki, S. Ando and M. Ueda, *Polymer Journal*, 2006, **38**, 79–84.
3. G. Maier, *Prog. Polym. Sci*., 2001**, 26**, 3-65.
4. C. Zhang, S. Guang, X. Zhu, H. Xu, X. Liu and M. Jiang, *J. Phys. Chem. C*., 2010, **114**, 22455–22461.
5. K. Su, D. R. Bujalski, K. Eguchi, G. V. Gordon, D. Li Ou, P. Chevalier, S. Hu and R. P. Boisvert, *Chem. Mater*., 2005, **17**, 2520-2529.
6. G. D. Fu, Y. Zhang, E. T. Kang and K. G. Neoh, *Adv. Mater*., 2004, **16**, 839-842.
7. S. Nunomura, K. Kog, M. Shiratani, Y. Watanabe, Y. Morisada1, N. Matsukil and S. Ikedal, Jpn. *J. Appl. Phys*., 2005, **44**, 1509-1511.
8. Z. Geng, J. Ba, S. Zhang, J. Luan, X. Jiang, P. Huo and G. Wang, *J. Mater. Chem*., 2012, **22**, 23534–23540.
9. S. Nagendiran, M. Alagar and I. Hamerton, *Acta Materialia*, 2010, **58**, 3345–3356.
10. Chyi-Ming Leu, Yao-Te Chang and Kung-Hwa Wei, *Macromolecules*., 2003, **36**, 9122-9127.
11. Md Abdul Wahab, Khine Yi Mya and Chaobin He, *J. Polym. Sci., Part A: Polym.Chem*, 2008, **46**, 5887–5896.
12. Chyi-Ming Leu, G. Mahesh Reddy, Kung-Hwa Wei and Ching-Fong Shu, *Chem. Mater*., 2003**, 15***,* 2261-2265.
13. Y. Chen, L. Chen, H. Nie and E.T. Kang, *J. Appl. Polym. Sci*., 2006, **99**, 2226–2232.
14. K. Zhang, Q. Zhuang, X. Liu, G. Yang, R. Cai and Z. Han, *Macromolecules*., 2013, **46**, 2696−2704.
15. Chu-Hua Lu, Shiao-Wei Kuo, Wen-Teng Chang and Feng-Chih Chang, *Macromol. Rapid Commun*., 2009, **30**, 2121–2127.
16. Yi-Che Su and Feng-Chih Chang, *Polymer*, 2003, **44**, 7989–7996.
17. M. R. Vengatesan, S. Devaraju, K. Dinakaran and M. Alagar, *J. Mater. Chem*, 2012, **22**, 7559–7566.

18. A. Chandramohan, K. Dinkaran, A. Ashok Kumar and M. Alagar, *High Perform. Polym*., 2012, **24**, 405–417.

19. S. Devaraju, M. R. Vengatesan, M. Selvi, A. Ashok Kumar, I. Hamerton, J. S. God and M. Alagar, *RSC Adv*. 2013, **3**, 12915–12921.

20. Ben-hong Yang, Hong-yao Xu, Zhen-zhong Yangc and Xiang-yang Liu, *J. Mater. Chem*., 2009, **19**, 9038–9044.

21. K. Zhang, Q. Zhuang, X. Liu, R. Cai, G. Yang and Z. Han, *RSC Adv*., 2013, **3**, 5261–5270.

22. J. Lin and X. Wang, *Polymer*, 2007, **48**, 318-329.

23. K. R. Carter, R. A. DiPietro, M. I. Sanchez and S. A. Swanson, *Chem. Mater*., 2001**, 13**, 213-221.

24. Hung-Cheng Liu, Wen-Chiung Sub and Ying-Ling Liu, *J. Mater. Chem*., 2011, **21**, 7182–7187.

25. Ying-Ling Liu and Meng-Han Fangchiang, *J. Mater. Chem*., 2009, **19**, 3643–3647.

26. Min-Chi Tseng and Ying-Ling Liu, *Polymer*., 2010, **51**, 5567-5575.

27. J. Choi, J. Harcup, A. F. Yee, Q. Zhu and R. M. Laine, *J. Am. Chem. Soc*., 2001, **123**, 11420-11430.

28. M. R. Vengatesan, S. Devaraju, K. Dinakaran and M. Alagar, *Polym. Compos*., 2011, **32**, 1701-1711.

29. T. Agag, C. R. Arza, F. H. J. Maurer and H. Ishida, *J. poly. Sci. part a: poly. chem*., 2011, **49**, 4335–4342.

30. J. Rathore, Q. Dai, B. Davis, M. Sherwood, R. D. Miller, Q. Linb and A. Nelson, *J. Mater. Chem*., 2011, **21**, 14254–14258.

31. Shiao-Wei Kuoa and Feng-Chih Chang, *Prog. Polym. Sci*., 2011, **36**, 1649–1696.

32. Yiwang Chena and En-Tang Kang, *Materials Letters*., 2004, **58**, 3716–3719.

33. Yuan-Jyh Leea, Jieh-Ming Huangb, Shiao-Wei Kuoa, Jian-Shing Lua and Feng-Chih Chang, *Polymer*., 2005, **46**, 173–181.

34. Ying-Ling Liu and Yi-Wen Chen, *Macromol. Chem. Phys*., 2007, **208**, 224–232.

35. Wen-Yi Chen, Ko Shan Ho, Tar-Hwa Hsieh, Feng-Chih Chang and Yen-Zen Wang, Macromol. *Rapid Commun*., 2006, **27**, 452–457.

36. H. Chen, L. Xie, H. Lu and Y. Yang, *J. Mater. Chem*., 2007, **17**, 1258–1261.

37. G. D. Fu, Z. Yuan, E. T. Kang, K. G. Neoh, D. M. Lai and A. C. H. Huan, *Adv. Funct. Mater*., 2005, **15**, 315-322.

38. C. H. Lin, S. J. Huang, P. J. Wang, H. T. Lin and S. A. Dai, *Macromolecules*, 2012, **45**, 7461−7466.